Density effect in K-hell ionization by ultrarelativistic electrons

PHYSICAL REVIEW A VOLUME 22, NUMBER 2 AUGUST 1980

Density effect in K-shell ionization by ultrarelativistic electrons

M. Kamiya and A. Kuwako
Department of Physics, Faculty of Science, Tohoku University, Sendai 980, Japan

K. Ishii and S. Morita
Cyclotron and Radioisotope Center, Tohoku University, Sendai 980, Japan

M. Oyamada
Laboratory of Nuclear Science, Faculty of Science, Tohoku University, Sendai 980, Japan

(Received 23 October 1978; revised manuscript received 21 January 1980)

Cross sections for K-shell ionization by 70- and 230-MeV-electron impact have been measured on the elements Na, Mg, Al, and Cl. Results for the lighter elements—Na and Mg—are smaller than the values predicted from the Kolbenstvedt theory and the plane-wave Born-approximation calculation. The rates of increase in the cross section with the increase in projectile energy from 70 to 230 MeV are also smaller than the predicted ones, and the cross section shows saturation at high bombarding energy. Furthermore, the increase rates of the cross section for lighter elements are compared with those for heavier elements by measuring relative x-ray yields with high accuracy on targets consisting of a pair of elements: (F,Al), (Na,Cl), (Mg,Mn), (Al,Mn), (Si,Mn), (Cl,Mn), and (Ca,Mn), and the increase rate for lighter elements is smaller than that for heavier elements except for the pairs (Cl,Mn) and (Ca,Mn). A similar result was obtained on the L-shell ionization of the pair (Zn,Sn). These results reveal the density effect in inner-shell ionization, which was predicted by Dangerfield, while the magnitude of the effect is not as large as that predicted from a simple theory. The discrepancy is discussed.

I. INTRODUCTION

Experimental studies of K-shell ionization by relativistic electrons have been reported by several authors,[1-4] and the results were interpreted by the virtual-photon theory of Kolbenstvedt,[5] by plane-wave Born approximation (PWBA) theories of Davidović and Moiseiwitsch,[6] and of Anholt,[7] and also by the fully relativistic PWBA of Scofield.[8] Good agreement between the experiments and the theories has been obtained, except for the experimental results obtained by Dangerfield and Spicer.[2]

On the other hand, Dangerfield[9] predicted the density effect in inner-shell ionizations by ultrarelativistic electrons. This effect has been well established in the ionization energy loss of a relativistic particle.[10,11] In an inner-shell ionization by relativistic electrons, as well as in the ionization energy loss, collisions of large impact parameter—distant collisions—are expected to make main contributions, so that a target atom can not be treated as an isolated one, but the effect of surrounding atoms should be taken into account. In the experimental results of Middleman *et al.*[1] obtained with 150–900-MeV electrons and in those of Ishii *et al.*[4] with 70–270-MeV electrons, however, no evidence of the density effect has been found even for lighter elements of Cu and Sr in the former experiment and of Al, Si, and Cl in the latter, within their experimental errors of about 40%.

In the present paper, K-shell ionization cross sections for light elements, where the density effect is expected to be more remarkable than for heavy elements, are measured and the results are compared with theories taking account of the density effect.

II. EXPERIMENT AND RESULTS

The experiment was made with the 300-MeV linear accelerator of Tohoku University. The general experimental setup was previously[4] reported and the parts relevant to the present measurement are described in detail. The experiment consists of two parts, measurement of absolute cross sections and of relative cross sections. In the former one, the absolute cross sections of K-shell ionization were measured on the targets of Na, Mg, Al, and Cl for electron energies of 70 and 230 MeV, and an increase rate of K-shell ionization cross section of Mn was also measured. The x rays from these targets were detected with a flow-type proportional counter of 2-μm aluminized Makrofol window. The Mn K x rays were measured with a Si(Li) detector of 160-eV energy resolution for 6.4-keV x rays. These detectors were shielded with 10-cm thick Pb blocks against γ rays. In order to avoid pileup due to the electron beam of 300 pulses/sec, counting rates had been kept below 10 counts/sec, so that correction for the pileup effect was about 2.5%. In these

TABLE I. Targets used, adopted values of fluorescence yield, ionization cross sections obtained at $E_e = 70$ and 230 MeV, and their ratios.

Target	Thickness ($\mu g/cm^2$)	ω_K	$\sigma^i(b)$ 70 MeV	230 MeV	σ^i(230 MeV)/σ^i(70 MeV)
Na	130.3	0.024	3500	3504	1.001 ± 0.058
Mg	273.2	0.0272	2644	2795	1.057 ± 0.040
Al	94.5	0.0357	2376	2547	1.072 ± 0.058
Cl	200.9	0.0942	1218	1296	1.064 ± 0.053
Mn					1.107 ± 0.033

measurements, elastically scattered electrons from the target were detected, since the beam current was too weak to be directly measured, and the integrated beam current was determined by comparing the counts of scattered electrons with those measured with a beam current of about 20 nA.

Targets of Na, Cl, and Mn were prepared by vacuum evaporation of sodium chloride and of Mn, respectively, onto 4-μm Mylar foils. Targets of Mg and Al were self-supporting. Thicknesses of these targets, except for the thickness of Mn, were measured by elastic scatterings of 3-MeV protons and ^{3}He particles, and are shown in Table I. Efficiency of the proportional counter was determined from the window transmission, which was measured by inserting the window material between the target and the counter. The intrinsic efficiency was calculated to be nearly unity, except for Cl K x rays, from the counter geometry and the photoionization cross section given by Storm and Israel.[12] The x-ray production cross sections obtained were converted into the ionization cross section using the values of fluorescence yield of Bambynek *et al.*[13] Total errors of the absolute cross section were estimated to be about 16% from the following errors: beam current, 3–4%; counting statistics, 1 ~ 4%; target thickness, ~10%; solid angle, ~5%; absorption in the target, 0 ~ 4%; and detection efficiency, 5 ~ 10%. Errors of the cross sections measured at 70 MeV relative to those at 230 MeV are 3–6%, which come only from uncertainties of beam current and counting statistics. Uncertainty in the fluorescence yield is not included in these errors. The results thus obtained are shown in Table I.

In the measurement of relative cross sections, the difference in increase rate of the cross sections from 70–230 MeV for a pair of elements has been measured on the eight targets consisting of a pair of elements: (F, Al), (Na, Cl), (Mg, Mn), (Al, Mn), (Si, Mn), (Cl, Mn), (Ca, Mn), and (Zn, Sn). The relative L-shell ionization cross sections have been measured for the target (Zn, Sn), and the difference in increase rate from 80–230 MeV was obtained for the target (Ca, Mn). The K x rays from the targets of (Si, Mn), (Cl, Mn), and (Ca, Mn) were detected with the Si(Li) detector and the others were with the proportional counter. In these experiments, counting rates have been kept at about 30 counts/sec. The targets of (F, Al) and (Na, Cl) were prepared by vacuum-evaporating AlF_3 and NaCl onto a thin organic film and a 4-μm Mylar film, respectively. The targets of (Mg, Mn), (Al, Mn), (Si, Mn), (Cl, Mn), and (Ca, Mn) were prepared by vacuum-evaporating Mn onto five Mylar films and Mg, Al, Si, NaCl, and Ca were then evaporated on each film. The calcium target was covered with a very thin Al layer by vacuum evaporation to prevent Ca from oxidation. The target of (Zn, Sn) was prepared by vacuum-evaporating Zn onto a self-supporting Sn foil.

The results of relative-cross-section measurements are shown in Table II. Small errors of 2–4% come only from counting statistics. The error due to background subtraction for the F x-ray peak from the (F, Al) target has been taken into account. Examples of the spectra obtained are represented in Fig. 1.

III. THEORIES

Theoretical calculations of K-shell ionization by relativistic electrons have been carried out in

TABLE II. Targets of a pair of elements, and ratios of the increase rate of ionization cross section from E_e = 70 to 230 MeV for the two elements.

Target	R	R(230 MeV)/R(70 MeV)
(F, Al)	F:Al	0.902 ± 0.035
(Na, Cl)	Na:Cl	0.941 ± 0.026
(Mg, Mn)	Mg:Mn	0.900 ± 0.027
(Al, Mn)	Al:Mn	0.923 ± 0.019
(Si, Mn)	Si:Mn	0.940 ± 0.035
(Cl, Mn)	Cl:Mn	0.999 ± 0.026
(Ca, Mn) [a]	Ca:Mn	1.021 ± 0.024
(Zn, Sn)	Zn:Sn	0.939 ± 0.029

[a] Increase rates from E_e = 80 to 230 MeV.

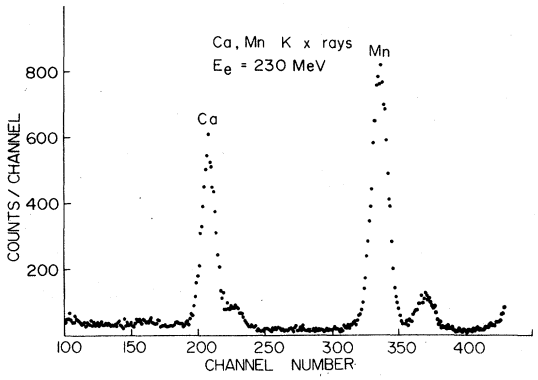

FIG. 1. K x-ray spectrum measured with the Si(Li) detector for a target of a pair of elements (Ca, Mn) bombarded with 230-MeV electrons.

terms of PWBA[6-8] and the virtual-photon method.[5] Both of the calculations are in good agreement with the experimental results. The virtual-photon method is used in this paper since it is capable of giving a clear physical concept with greater ease than the PWBA. The ionization cross section can then be divided into two parts:

$$\sigma^{\mathrm{tot}} = \sigma^{\mathrm{close}} + \sigma^{\mathrm{dist}}, \tag{1}$$

where σ^{close} corresponds to the ionization by collisions of impact parameter b smaller than the K-shell radius a and the collision time is shorter than the K-shell electron period. Then the ionization can be considered to take place by a collision between two free electrons with an energy transfer greater than the electron-binding energy. If the atomic electron is assumed to rest, the Møller formula gives[14] (in barns)

$$\sigma^{\mathrm{close}} = \frac{0.99}{I}\frac{(E+1)^2}{E(E+1)}\left[1-\frac{I}{E}\left(1-\frac{E^2}{2(E+1)^2}+\frac{2E+1}{(E+1)^2}\ln\frac{E}{I}\right)\right], \tag{2}$$

where I and E are, respectively, the binding energy of the K-shell electron and the kinetic energy of the incident electron, expressed in units of the electron-rest mass.

The cross section for distant collisions σ^{dist} corresponds to ionizations due to collisions of $b > a$ and is calculated from the virtual-photon method: The rapidly varying field produced by an incident electron at the position of the atom to be ionized is expressed by a virtual-photon spectrum, which gives rise to the ionization by the photoeffect. This virtual-photon spectrum is expressed by[15]

$$\frac{dN(\hbar\omega,b)}{dbd(\hbar\omega)} = \frac{2\pi b}{\hbar\omega}\frac{1}{\pi^2}\frac{e^2}{\hbar c}\left(\frac{c}{v}\right)^2\frac{1}{b^2}\left[\left(\frac{\omega b}{\gamma v}\right)^2 K_1^2\left(\frac{\omega b}{\gamma v}\right)+\frac{1}{\gamma^2}\left(\frac{\omega b}{\gamma v}\right)^2 K_0^2\left(\frac{\omega b}{\gamma v}\right)\right], \tag{3}$$

where $\hbar\omega$, $\gamma = 1/[1-(v/c)^2]^{1/2}$, v, and e are the photon energy, the incident-electron energy expressed in units of the rest mass, the velocity and charge of the incident electron, respectively; K_0 and K_1 are the zero-th and the first-order modified Bessel functions of the third kind. This spectrum is shown Fig. 2, where N_1 and N_2 represent the first and the second terms, respectively, in the bracket of Eq. (3).

As seen in Fig. 2 and Eq. (3), collisions of impact parameter of $b < \gamma v/\omega$ make a main contribution to the ionization. For example, we obtain $b_{\max} \approx 80$ Å for $\hbar\omega = 5$ keV and $E_e = 100$ MeV, and for a collision of such a large impact parameter, the effect of medium surrounding the target atom should not be neglected.

Integrating Eq. (3) over the region $b > a$ and using the relation $\omega \ll \gamma v/a$, we can approximately obtain

$$\frac{dN(\hbar\omega)}{d(\hbar\omega)} = \frac{2}{\pi}\frac{e^2}{\hbar c}\left(\frac{c}{v}\right)^2\frac{1}{\hbar\omega}\left[\ln\left(\frac{1.123\gamma v}{\omega a}\right)-\frac{v^2}{2c^2}\right]. \tag{4}$$

The ionization cross section for virtual photons can then be expressed (in barns)

$$\sigma^{\mathrm{dist}} = \int_I^{\hbar\omega_{\max}} \sigma^{\mathrm{photo}}(\hbar\omega)\frac{dN(\hbar\omega)}{d(\hbar\omega)}d(\hbar\omega) = 0.77\frac{I_0^3}{\beta^2}\int_{I_0\theta}^{\hbar\omega_{\max}} d(\hbar\omega)\frac{1}{(\hbar\omega)^5}\frac{4\hbar\omega - I_0}{3I_0}\times[\ln(2\gamma^2 v^2 I_0/\omega^2)-\beta^2], \tag{5}$$

where $\omega_{\max}$ is the value of ω which gives Eq. (4) $= 0$, $I_0 = \frac{1}{2}(\alpha Z_{\mathrm{eff}})^2$, and θ is the screening factor. As Kolbenstvedt did, the factor 2 in the last term of Eq. (5) was taken instead of 2(1.123). Using the photoeffect cross section given by Stobbe,[16] and carrying out the integration, we obtain (in barns)

$$\sigma^{\mathrm{dist}} = \frac{0.278}{I\theta^3}\frac{1}{\beta^2}\{[1-\tfrac{16}{13}(1-\theta)][\ln(2\gamma^2\beta^2/I)-\beta^2]-\tfrac{55}{78}+\tfrac{32}{39}(1-\theta)\} \tag{6}$$

$$= \frac{0.278}{I\theta^3}\frac{(E+1)^2}{E(E+2)}\left\{[1-\tfrac{16}{13}(1-\theta)]\left[\ln\left(\frac{2E(E+1)}{I}\right)-\frac{E(E+1)}{(E+1)^2}\right]-\tfrac{55}{78}+\tfrac{32}{39}(1-\theta)\right\}. \tag{7}$$

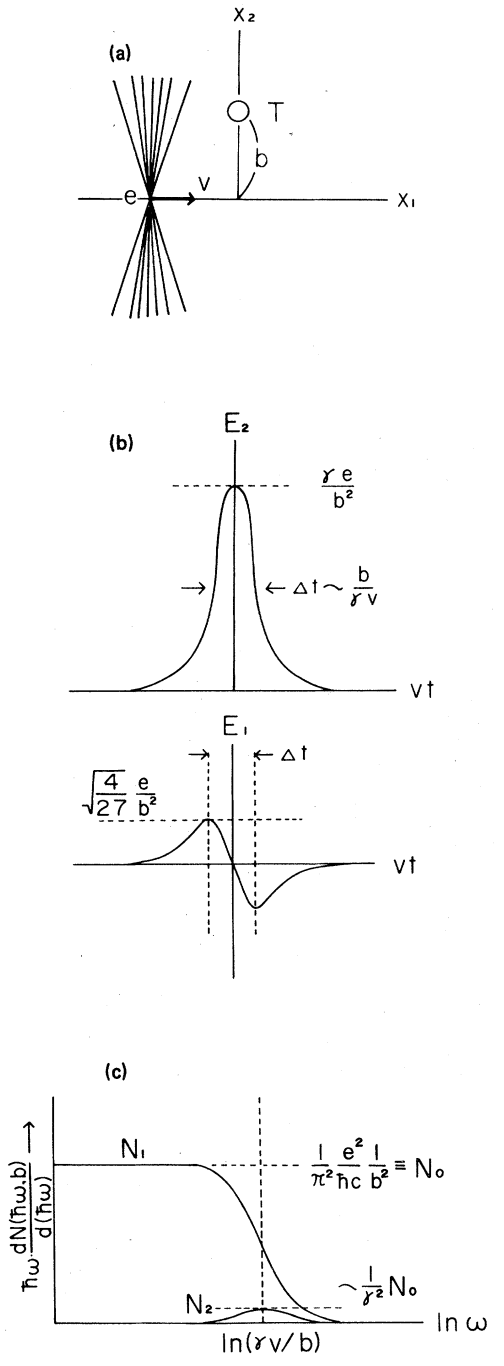

FIG. 2. (a) An electron comes in the direction X_1 with velocity v, and lines of electric force for the electron concentrate in the direction vertical to the velocity. (b) The target atom suffers an electric pulse of time duration Δt; E_1 and E_2 are the components in the directions X_1 and X_2, respectively. (c) The pulse is expanded in terms of the frequency ω the virtual-photon spectrum. The notations N_1 and N_2 are the photon number multiplied by $\hbar\omega$, corresponding to E_2 and E_1, respectively.

Next, the effect of medium around the target atom is to be considered. Atoms surrounding the target atom to be ionized are polarized by the field produced by an incident particle, and this effect is classically taken into account by the dielectric constant ϵ of the medium. The density effect in ionization cross sections is brought into consideration by replacing the phase velocity of light c in Eqs. (5) and (6) with $c/\sqrt{\epsilon}$, and as seen in Fig. 2, this effect gives rise to decrease in the maximum impact parameter contributing to the ionization and becomes important for collisions of large impact parameter.

All the electrons can be considered to be free for photons of $\hbar\omega > I$, which is needed for the ionization. Moreover, if the wavelength of the virtual photon is assumed to be large in comparison with the interatomic distance, the dielectric constant is expressed by[17]

$$\epsilon(\omega) = 1 - \omega_p^2/\omega^2 , \tag{8}$$

with $\omega_p^2 = 4\pi ne^2/m$, where n is the total electron density, ω_p is called the plasma frequency and m is the electron mass.

Though there is some doubt whether or not a macroscopic quantity such as the dielectric constant is applicable to an x-ray region, where the wavelength is comparable to the lattice constant of medium, it has been well confirmed experimentally that Eq. (8) is valid for physical quantities such as refractive index and is applicable even to an x-ray region. On the other hand, it must be pointed out that we are here concerned with virtual photons, not with real photons. An electric pulse of time duration Δt, shown in Fig. 2, is expanded as a function of frequency. Hence, a virtual photon of energy $\hbar\omega$ consists of pulses of duration Δt smaller than $1/\omega$. The extent of electromagnetic field of these pulses is of the order of magnitude of $c\Delta t$ and coherent scattering contributing to the dielectric constant are also confined in this region.

It can be considered that a photon would not propagate in a medium with the velocity $c/\sqrt{\epsilon}$, if the size of medium were smaller than a certain limit—say, V. So that, if the extent of a virtual photon $(c\Delta t)^3$ is smaller than the limit V, Eq. (8) would no longer be valid. Considering that the intensity of a scattered wave is to be multiplied by a factor $(c\Delta t)^3/V$ and the wavelength of the virtual photon is $\lambda \approx c\Delta t$, we put $V = (hd)^3$, where h is a parameter and d is the lattice constant of the medium; hd might be several tens of Å.

Thus the dielectric constant for virtual photons can be expressed by

$$\epsilon(\omega) = 1 - \frac{\omega_p^2}{\omega^2}\left(\frac{\lambda}{hd}\right)^3 , \tag{9}$$

with $\epsilon(\omega) = 1 - \omega_p^2/\omega^2$ for $(\lambda/hd)^3 \geq 1$. Corresponding to Eq. (8), we will define the effective plasma frequency by

$$\tilde{\omega}_p^2(\omega) \equiv \omega_p^2(\lambda/hd)^3 ,$$

and we can write

$$\epsilon(\omega) = 1 - \tilde{\omega}_p^2(\omega)/\omega^2 . \qquad (10)$$

IV. DISCUSSION

The experimental ionization cross sections for Na, Mg, Al, and Cl are illustrated in Figs. 3(a)–3(d), together with the theoretical predictions. The solid and the dashed lines represent, respectively, the PWBA[7] and the Kolbenstvedt theories. The experimental results are a little smaller than the theories, and this fact suggests contribution from the density effect. The calculated cross sections, taking into account the density effect by using the dielectric constant given by Eqs. (9) or (10), are shown by thin curves in Fig. 3, where the parameter was taken as $h = 10.0$ and the values of the plasma frequency ω_p and the lattice constant, or interatomic distance, used in this calculation are shown in Table III. As seen in these figures, the discrepancy between the theories and the experiment is a little improved by taking account of the density effect. The contribution from the effect, however, is not conclusive because of the experimental error of ~16%, and also because of the errors in the fluorescence yield.

The K-shell ionization cross sections obtained at $E_e = 70$ MeV are compared with the PWBA theory in Fig. 4, together with the data obtained by Ishii *et al.*[4] and by Hoffmann *et al.*[3] The results of Hoffmann *et al.* were estimated from extrapolation of the results for 20–60 MeV. The present results on light elements are quite consistent with the others. The K-shell ionization cross sections obtained at $E_e = 230$ MeV are shown as a function of the atomic number and are compared with the theories in Fig. 5. It is seen in this figure that the experimental results on light elements at 230 MeV are smaller than the theories.

TABLE III. Values of the plasma frequency and the lattice constant, or interatomic distance, used for estimating the density effect from Eqs. (9) and (10).

Matter	$\hbar\omega_p$ (eV)	d(Å)
AlF_3	35.00	1.780
NaCl	29.37	1.770
Mg	26.00	1.425
Al	32.79	1.275
Si	31.04	1.360
Ca	25.33	1.750
Mn	52.18	1.165
Cu	58.15	1.140

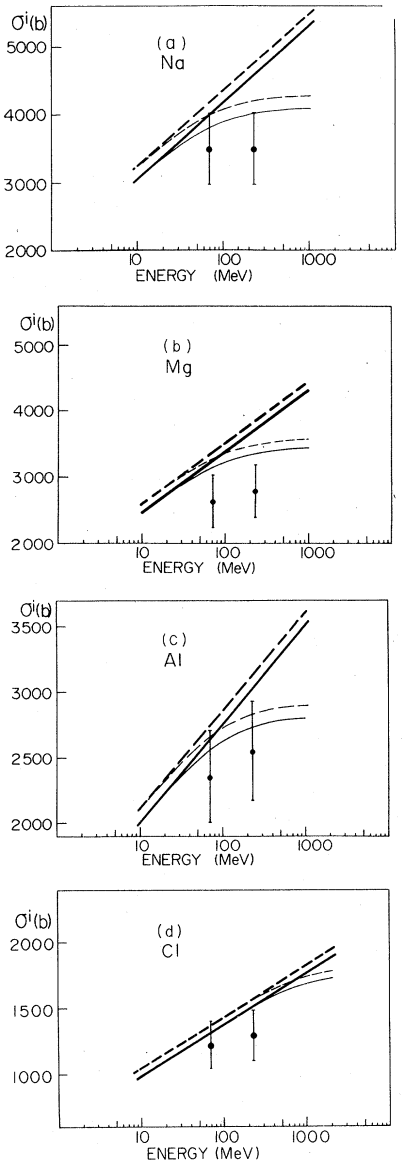

FIG. 3. The K-shell ionization cross sections for (a) Na, (b) Mg, (c) Al, and (d) Cl. The solid and the dashed lines are calculated, respectively, from PWBA and the Kolbenstvedt theories. The thin curves are obtained including the density effect using the effective dielectric constant given by Eq. (10) in the text. The experimental points are for $E_e = 70$ and 230 MeV.

Apart from the absolute cross-section measurement with large errors, we will discuss more precise measurement of the increase rate. Figure 6 shows the x-ray spectra for the NaCl target obtained at $E_e = 70$ and 230 MeV. A small shift of the peak positions is due to a difference of 20 V in the high voltage applied to the proportional

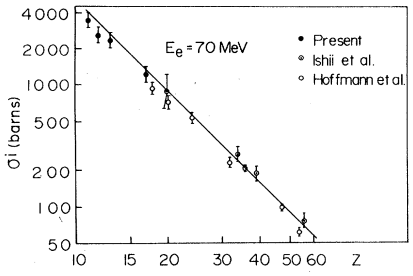

FIG. 4. Experimental results on K- shell ionization cross section obtained at $E_e = 70$ MeV, including the results previously obtained, are compared with the PWBA calculation (the solid line).

counter. Other conditions for the measurement are the same for the two bombarding energies. It is seen in this figure that, although the height of Cl peak is about the same for the two bombarding energies, the Na peak for 230 MeV is clearly smaller than that for 70 MeV. This fact shows saturation in cross section for Na—the lighter element.

The increase rate of ionization cross section corresponding to the increase in incident energy from 70 to 230 MeV is illustrated in Fig. 7, where the experimental results are evidently smaller than the theoretical rate of about 15%. The closed circles in this figure were obtained from the absolute measurements, while the open circles were from the measurements relative to Mn with errors of 2–3%. The fact that the values of open circle are somewhat smaller than those of closed circle may be due to a small value of 11% for the increase rate of Mn. If we take a theoretically predicted value of 15% instead of 11%, the differences between the closed and open circles for Mg and Al are removed. The dashed line in Fig. 7 does not take the density effect into consideration, the solid line was obtained by taking into account the density effect using the dielectric constant of Eq. (10), and the dotted line is obtained by using the dielectric constant of Eq. (8). The theoretical values shown here are calculated from the Kolbenstvedt theory, but as can be seen in Fig. 3, the PWBA calculations give the same results. It is understood from this figure that the increase rate for $Z \leq 14$ becomes substantially smaller than the value predicted without the density effect, though there is no conclusive evidence on the effect in region $Z \geq 20$. Moreover, the value calculated using the effective plasma frequency $\bar{\omega}_b(\omega)$ can well reproduce all the experimental values. The experimental results on the K-shell ionization of Cu, obtained by Middleman *et al.*,[1] are compared with theoretical predictions in Fig. 8, where the dashed and the solid lines stand for the Kolbenstvedt theory and the PWBA, respectively, and the thin curves show the density effect estimated using the effective dielectric constant. It is quite understandable from Fig. 8 that the density effect becomes observable in the region beyond ~2000 MeV, and not in the region below 900 MeV.

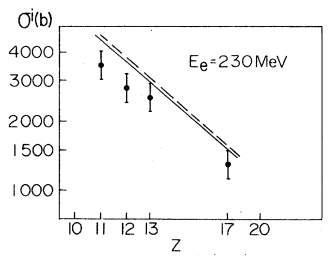

FIG. 5. Comparisons of the present results obtained at $E_e = 230$ MeV with predictions from the PWBA (solid line) and the Kolbenstvedt theory (dashed line).

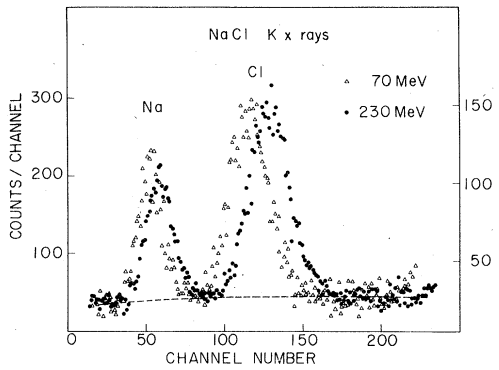

FIG. 6. Comparison of the x-ray spectrum for a NaCl target obtained at $E_e = 70$ MeV with that obtained at $E_e = 230$ MeV. The Na peak for 230 MeV is definitely smaller than that for 70 MeV, while the Cl peaks for the two projectile energies are about the same. The right-hand scale is for 70 MeV, and the left is for 230 MeV.

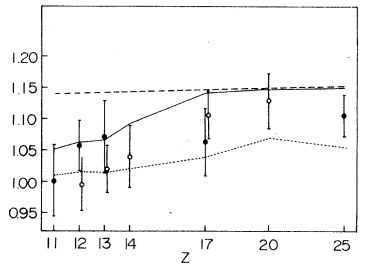

FIG. 7. The ratio of ionization cross sections obtained at the two projectile energies versus the atomic number of target. The dashed line is the theoretical prediction without the density effect. The solid and the dotted lines are calculated by taking into account the density effect using the dielectric constant given by Eqs. (10) and (8), respectively, in the text. These lines connect the theoretical values only as a guide to the eye.

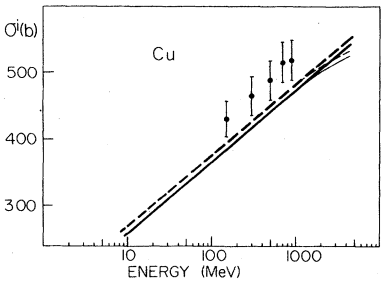

FIG. 8. The K-shell ionization cross sections of Cu obtained by Middleman *et al.* are compared with theories (solid line—PWBA and dashed line—the Kolbenstvedt theory). The thin curves show the density effect using the effective dielectric constant given by Eq. (10).

If we define the ratio of x-ray yields from two elements at a bombarding energy as R, then a quantity defined by

$$\frac{R(E_1)}{R(E_0)}=\frac{Y_A(E_1)/Y_B(E_1)}{Y_A(E_0)/Y_B(E_0)}=\frac{\sigma_A(E_1)/\sigma_A(E_0)}{\sigma_B(E_1)/\sigma_B(E_0)}$$

represents the ratio of the increase rate from $E_e=E_0$ to E_1 for the two elements—A and B. If the density effect does not exist, the increase rate for the two elements is approximately the same: $R(E_1)/R(E_0)\approx 1$. On the other hand, if the density effect appears only in A or more strongly in A, it then becomes $R(E_1)/R(E_0)<1$. Ratios of the increase rate of the K x-ray yield between two elements of the pairs (F, Al), (Na, Cl), (Mg, Mn), (Al, Mn), (Si, Mn), (Cl, Mn), and (Ca, Mn), and ratios of the L x-ray yield for a pair of (Zn, Sn) are shown in Table II and Fig. 9, where the fact that the increase rates for light elements are smaller than those for heavy elements evidently reveals the

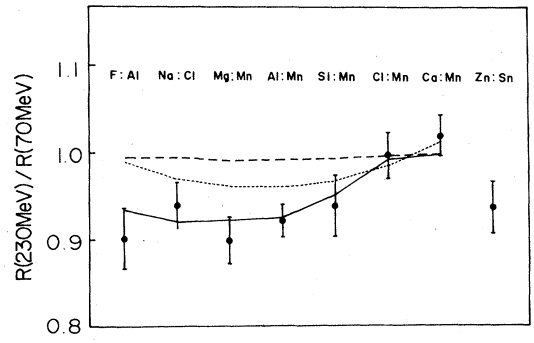

FIG. 9. Ratios of increase rate of ionization cross section from $E_e=70$ to 230 MeV between the pair of elements making a target. The dashed line is the prediction from the Kolbenstvedt theory. The solid and the dotted lines were calculated by taking into account the density effect using the effective dielectric constant of Eq. (10) and the usual dielectric constant of Eq. (8), respectively. These lines connect the theoretical values only to guide the eye.

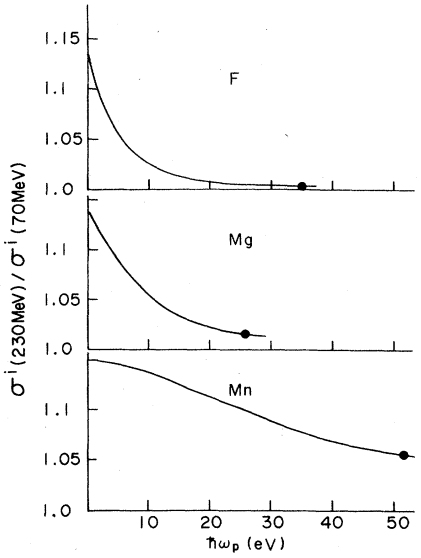

FIG. 10. Ratios of the K-shell ionization cross section obtained at $E_e=230$ MeV to those obtained at 70 MeV are plotted as a function of the plasma frequency.

contribution of the density effect. The theoretical values are calculated from the Kolbenstvedt theory; the horizontal dashed line without the density effect, the solid line taking into account the effect using the effective dielectric constant of Eq. (10), and the dotted line with the dielectric constant given by Eq. (8). As seen in this figure, the density effect using the effective dielectric constant gives the best fit to the experimental results. An attempt was made to fit the experimental results by adjusting the plasma frequency ω_p given by Eq. (8). Figures 10 and 11 show the

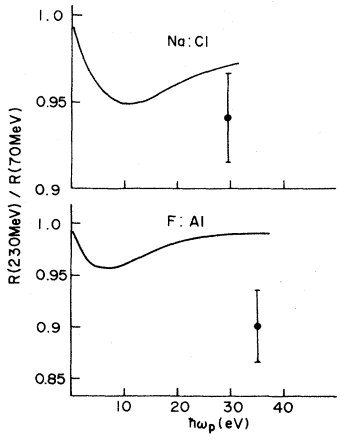

FIG. 11. Ratio of increase rate of the cross sections between the two elements making a target is plotted as a function of the plasma frequency. The upper curve is for the NaCl target and the lower one is for the AlF_3 target.

ratio of increase rate as a function of ω_p, and in Fig. 11, one value of ω_p should be taken for each of the pairs, since the targets of aluminum fluoride and sodium chloride have been used. Nevertheless, it is difficult to reproduce the experimental values as seen in Fig. 11. L-shell ionizations have been measured for a pair of (Zn, Sn), and as seen in Fig. 9, saturation is found in the lighter element Zn as in the case of K-shell ionization.

V. SUMMARY

The experimental results on inner-shell ionization by ultrarelativistic electrons, previously obtained on medium and heavy elements, have been in good agreement with the PWBA and Kolbenstvedt theories and have shown no evidence for the density effect, which was pointed out by Dangerfield and has been well established in the ionization energy loss.

In this paper, K-shell ionization cross sections for electron impact on light elements—Na, Mg, Al, and Cl—have been measured at incident energies of 70 and 230 MeV, and the difference in the increase rate of the cross section from 70 to 230 MeV was also measured for pairs of elements (F, Al), (Na, Cl), (Mg, Mn), (Al, Mn), (Si, Mn), (Cl, Mn), and (Ca, Mn). Difference in the increase rate of L-shell ionization cross sections was measured for a pair of (Zn, Sn).

For light elements such as Na and Mg, both of the cross sections and the increase rates are smaller than the theoretical prediction. Moreover, differences between the increase rate for light elements and that of heavier elements demonstrates definitely the saturation of cross section for light elements, and it was also found that the saturation for heavier elements is not so remarkable as was expected by Dangerfield: No saturation was observed in the elements heavier than Ca. By assuming the corrected dielectric constant for virtual photons, satisfactory agreement with the experimental results could be obtained and the explanation which is consistent with the results previously obtained was also obtained. The incident energy is quite limited in the present measurements. It is desirable to extend the measurement to higher bombarding energies.

ACKNOWLEDGMENT

The authors wish to express their appreciation to the staff of the Laboratory of Nuclear Science, Tohoku University, for operating the linear accelerator throughout the work.

[1] L. M. Middleman, R. L. Ford, and R. Hofstadter, Phys. Rev. A 2, 1429 (1970).
[2] G. R. Dangerfield and B. M. Spicer, J. Phys. B 8, 1744 (1975).
[3] D. H. H. Hoffmann, H. Genz, W. Löw, and A. Richter, Phys. Lett. A 65, 304 (1978), and private communication.
[4] K. Ishii, M. Kamiya, K. Sera, S. Morita, H. Tawara, M. Oyamada, and T. C. Chu, Phys. Rev. A 15, 906 (1977).
[5] H. Kolbenstvedt, J. Appl. Phys. 38, 4785 (1967). See also Ref. 1.
[6] D. M. Davidović and B. L. Moiseiwitsch, J. Phys. B 8, 947 (1975).
[7] R. Anholt, Phys. Rev. A 19, 1004 (1979).
[8] J. H. Scofield, Phys. Rev. A 18, 963 (1978).
[9] G. R. Dangerfield, Phys. Lett. A 46, 19 (1973).
[10] A. Crispin and G. N. Fowler, Rev. Mod. Phys. 42, 290 (1970).
[11] R. M. Sternheimer, Phys. Rev. 88, 851 (1952).
[12] E. Storm and H. I. Israel, Nucl. Data Sec. A 7, 565 (1970).
[13] W. Bambynek, B. Crasemann, R. W. Fink, H. U. Freund, H. Mark, C. D. Swift, R. E. Price, and P. Venugopala Pao, Rev. Mod. Phys. 44, 716 (1972).
[14] J. M. Jauch and F. Rohrlich, *The Theory of Photons and Electrons* (Addison-Wesley, Cambridge, Mass., 1954), p. 256.
[15] J. D. Jackson, *Classical Electrodynamics* (Wiley, New York, 1975), 2nd ed.
[16] W. Heitler, *Quantum Theory of Radiation* (Oxford University Press, London, 1954), 3rd ed.
[17] E. Burstein, *Dynamical Processes in Solid State Optics*, 1966 Tokyo Summer Lectures in Theoretical Physics, edited by R. Kubo and H. Kamimura (Syokabo, Tokyo, and Benjamin, New York, 1967), p. 1.